

Transition to Turbulence through Intermittence in Inert and Reacting Jets

V. V. Lemanov^{a,*}, V. V. Lukashov^a, and K. A. Sharov^a

^a*Kutateladze Institute of Thermophysics, Siberian Branch of the RAS,
ul. Akademika Lavrentyeva 1, Novosibirsk, 630090 Russia*

**e-mail: lemanov@itp.nsc.ru*

Received February 3, 2020; revised March 5, 2020; accepted March 12, 2020

Abstract—Subsonic flows of different gases in the near field of inert and reacting jets is experimentally investigated. The jets flowed out of long tubes, 2 to 8 mm in diameter, into an air medium at low Reynolds numbers from 400 to 5000. The working fluids were air, carbon dioxide, propane, and Freon-22 for inert isothermal jets and propane mixed with an inert dilution (CO₂) for reacting jets. The tools included Hilbert visualization, PIV, hot-wire anemometry, and probe thermometry. A scenario of transition to turbulence through the intermittence mechanism in inert and reacting jets is revealed for the first time. It is realized in the Reynolds number range from 1900 to 3500, when laminar-turbulent transition occurs within the jet source, that is, the tube, in the absence of artificial disturbances. Turbulent spots generated in the tube in the transitional regime are statistical in nature and fairly stable in the jet near-field. Propagating downstream they can have a considerable effect on the dynamics of free jets and diffusion plumes.

Keywords: subsonic gas jets, laminar-turbulent transition, intermittence, vortex structures, diffusion combustion

DOI: 10.1134/S0015462820060087

Laminar-turbulent transition in subsonic jets has been studied fairly extensively from both theoretical and experimental points of view [1–8]. It is the instability of jets issuing from contoured nozzles of conusor type at large Reynolds numbers ($Re > 10^4$) that was chiefly investigated. This formulation of the problem is due to the great practical use of jets flowing out of nozzles. In this case, the initial velocity profile is of the “top-hat” type, with thin boundary layers. In these flows, laminar-turbulent transition is realized in the mixing layer within the initial jet region ($x/d = 4–8$). In this zone, the linear mechanism of disturbance growth associated with Kelvin—Helmholtz instability passes rapidly to the nonlinear stage related with the phenomenon of pairwise vortex coalescence. In the spectral representation this is interpreted as the appearance of subharmonic frequencies [3, 9]. At the same time, in practice jets can frequently flow out of long channels, for examples, in burners [10]. It is known that initial conditions can play a considerable role in the development of subsonic jet flows [1–6, 11–14].

So far, the instability of jets issuing from long channels has not been adequately studied, particularly, at nonlinear development stages. As shown in [11, 12], in these jets the coordinate of transition to turbulence can achieve such large values, as $x/d = 200–500$. It was found that in the Reynolds number range from 2000 to 3000 this coordinate can considerably diminish [12]. It is known that at these Reynolds numbers in long cylindrical channels transition to turbulence is possible with the formation of vortex structures of the type of puffs and slugs [15–17].

In considering diffusion combustion in jets different flow patterns can be encountered, such as attached and detaches flames, laminar and turbulent flows, and regimes with flame-out [10]. The experiments on the combustion in the case of outflow from long tubes showed that the transition processes in the channel considerably influence the plume dynamics [18, 19]. For this reason, there arose the problem of investigating transition in inert and reacting jets under the conditions of laminar-turbulent transition development in the jet source. In this study, much attention is also given to the large vortex structures that exist in these regimes in the jet near-field.

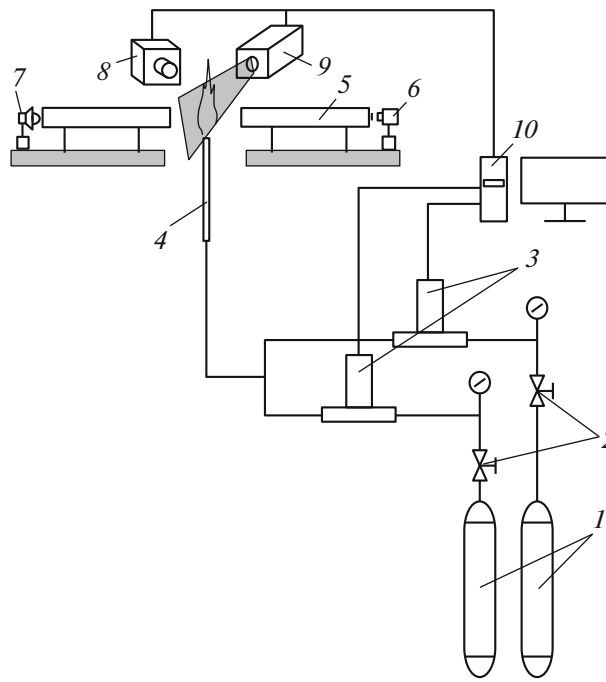


Fig. 1. Schematic of the experimental setup; 1, gas reservoirs; 2, gas pressure regulators; 3, digital flowmeters; 4, tube; 5, shadow instrument equipped with the Hilbert optics; 6, digital camera; 7, light source; 8, high-speed digital camera; 9, pulsed high-speed laser; and 10, computer.

1. EXPERIMENTAL SETUP AND MEASUREMENT TECHNIQUES

In this study, several experimental methods are used. These are visualization using the Hilbert optics, high-speed Particle Image Velocimetry (PIV), hot-wire anemometry, and measurements in flames with a temperature probe. Both isothermal flow (air, Freon-22 (CHF_2Cl), CO_2 , and propane C_3H_8) and diffusion flames (C_3H_8 mixed with CO_2) were investigated. The gas-mixture jets flowed out into an open air space under the atmospheric pressure.

The experimental setup (Fig. 1) consisted of gas reservoirs (1), gas pressure regulators (2), two digital flowmeters (3), and a jet source (4). The gas flow rate and the combustion mixture composition were determined using digital El-Flow Bronkhorst and UFGS-2 flowmeters. The gas mixture viscosity required in the calculations was estimated according to the Sutherland model in the Wilke approximation [20]. The Hilbert optics [21, 22], which is a high-sensitive visualization method of optical density fields, was used in experimentally investigating reacting flows disturbed by vortex structures. For this purpose, the production-type IAB-463M shadow instrument (5) additionally equipped with the Hilbert optics was used. Shearing interferograms [21] and jet flame visualization were recorded using the Canon 650D digital camera (6) with the filming speed of 50 frames per second.

The PIV system for measuring velocity fields included the Photron SA5 camera (8) with the temporal resolution of 7 kHz. The flow was seeded with light-scattering particles using an aerosol generator (absent from the figure) joined up to the feeding manifold after the flowmeters (6). The aerosol is the suspension of glycerin droplets, about 1 to 2 μm in size. The laser knife was formed using a pulsed high-speed Nd : YAG DM-532-50 laser (9) with the burst repetition frequency to 10 kHz and the pulse power of 10 mJ. The data were gathered by a computer (10). The images of the light-scattering particles obtained by the high-speed camera were processed using the algorithms of the ActualFlow code [23]. This made it possible to obtain the fields of instantaneous values of the axial and radial velocity components in a 80×70 mm region.

The dynamic characteristics were measured with a constant-temperature hot-wire DISA 55M anemometer. A tiny DISA 55P11 probe was used as a sensor (golden tungsten, wire diameter of 5 μm , and wire length of 0.6 mm).

The gas temperature at the entry into the test section was measured with a digital Ebro TFX392L thermometer. The temperatures in the plume were measured with TPR-0392-01 Pt/Pt-Rh-thermocouple with wires, 120 μm in diameter. In this study, any correction of the temperature measurements was not

performed. A 24-digit LTR114 AD converter having the maximum discretization frequency of 4 kHz was used for gathering the hot-wire and temperature data and saving them on a computer hard disk.

The jet flow was formed using round tubes, $d = 2\text{--}8$ mm in the inside diameter and $l/d = 200\text{--}300$ in length. In hot-wire measurements the jet flowed out in a $150 \times 150 \times 300$ space bounded by a flow-through channel made of Plexiglas. In the case of PIV measurements of the dynamic flow characteristics the outflow occurred into an analogous $400 \times 400 \times 400$ mm channel. No artificial disturbances were introduced in the flow (both within the tube and in the jet).

2. NONREACTING JETS

Since the initial conditions play a considerable role, in studying inert free jets much attention was given to the conditions at the exit from the cylindrical channel. In Fig. 2a the dependence of the velocity ratio U_0/U_m and the turbulence level ($Tu = u/U_0 \times 100\%$) at the channel axis on the Reynolds number is presented for $x = 0.3$ mm. Here, U_0 is the gas velocity in the tube exit section at the axis, U_m is the mean-flow-rate gas velocity through the tube, u is the r.m.s. value of velocity fluctuations, and x is the longitudinal coordinate measured from the tube end. As can be seen in the figure, the velocity ratio varies from $U_0/U_m = 2$ corresponding to the laminar Poiseuille profile to $U_0/U_m = 1.25$ characteristic of the developed profile of turbulent tube flow. This variation is due to laminar-turbulent transition of the gas flow in the tube in the $Re = U_m d/\nu = 2511\text{--}2625$ range. In the transitional region the turbulence level Tu has a local extremum at $Re = 2620$; in this case, a maximum fluctuation level, $Tu = 15.2\%$, is reached. In the experiments, an intermittent regime, that is, the alternation of laminar and turbulent flow regions, is observable.

At the second stage the measurements at the gas jet axis were performed by the hot-wire anemometer at variation of the Reynolds number Re from 460 to 4092. In Fig. 2b the dependence of the turbulence level on the dimensionless distance x/d is plotted. In accordance with the initial data presented in Fig. 2a, three groups of characteristic curves can be established. Thus, 1 to 3 correspond to the Reynolds numbers $Re = 460\text{--}1970$, that is, to the laminar flow regime in the jet source (tube); 4 relates to $Re = 2620$ corresponding to laminar-turbulent transition regime in the tube; and 5 and 6 correspond to the Reynolds numbers $Re = 2810\text{--}4092$, that is, to the turbulent flow regime in the tube. Depending on the tube flow nature, some characteristic regimes of jet propagation can be established. Thus, regime A corresponds to laminar flow in the tube. For jets with low Reynolds numbers ($Re = 460$) typical is an extended laminar flow zone (up to $x/d = 30$) with a low level of velocity fluctuations. It is followed by a laminar-turbulent transition region, where fluctuations grow and then by a turbulent flow zone, where fluctuations diminish. With increase in the Reynolds number the length of the laminar jet region reduces, while the fluctuation maximum in the transitional region increases. At $Re = 1970$ the laminar zone length $x/d = 12$ and the fluctuations reach the value $Tu = 21\%$. Regime B corresponds to laminar-turbulent transition in the tube. At $Re = 2620$ the velocity fluctuation level at the axis in the initial jet section increases sharply and reaches a maximum value $Tu = 15.2\%$. As a result, the fluctuations in the jet near-field sharply increase (up to $Tu = 30\%$ at $x/d = 7$). Finally, regime C corresponds to turbulent flow in the tube. With further increase in the Reynolds number ($Re = 2810\text{--}4092$) the initial fluctuation level decreases to $Tu = 3.3\%$, while their maximum at $x/d = 7$ decreases to $Tu = 10\%$. Further downstream ($x/d > 10$) the velocity fluctuations are considerably reduced, which indicates a strong dissipation of the turbulent energy in this region.

The flow visualization in inert jets was carried out for air, Freon-22, and propane. For regime B the regime with intermittence, that is, the alternation of laminar and turbulent flow regions is observable in the tube and the near region of gas jets. In Fig. 3 the Hilbert visualization of Freon-22 jet in the air is presented; the flow is from the top down. The jet beginning corresponds to the tube end. Two successive frames of the movie made with the shooting frequency of 50 frames per second are presented. The Reynolds number $Re = 2853$, which corresponds to the range of laminar-turbulent transition in the tube. In Fig. 3a an extended laminar flow region can be seen, together with transition to turbulent flow at the end of the frame. This is the laminar flow stage in the near region of the jet. In Fig. 3b the turbulent flow stage is presented. In the first (top) half of the frame a local turbulent formation (puff) can be observable; its length is of the order of $20d$ and it occupies the entire jet cross-section. This intermittent flow pattern was obtained for all the gases considered, namely, air, Freon-22, and propane.

The experiments showed that the internal structure of the turbulent spot in the jet is fairly complicated. The mechanism of formation of these local spots in tubes has been adequately elucidated in the modern literature [15–17]. The structures of two types are distinguished, namely, puffs and slugs. The former structures are generated at the Reynolds numbers characteristic for laminar-turbulent transition and the

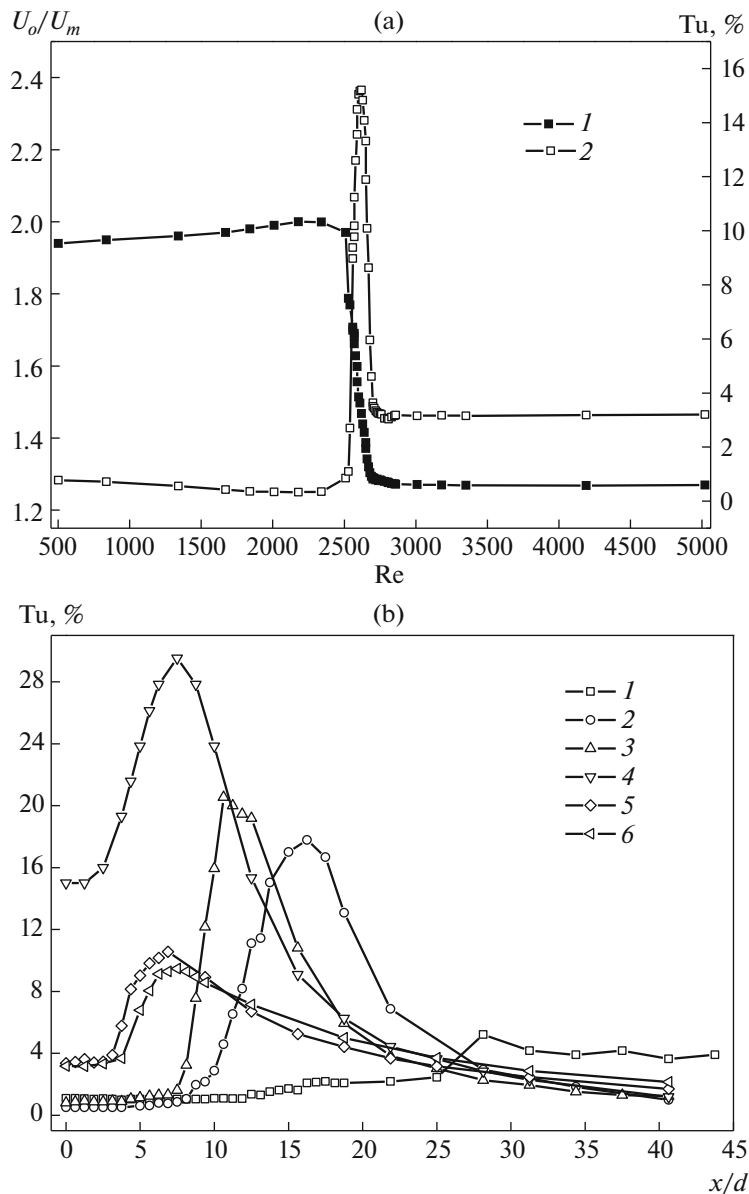


Fig. 2. Parameter distributions in the air jet, $d = 3$ mm. (a) Dependence of the velocity ratio and the turbulence level on the Reynolds number at the tube exit; 1, U_0/U_m and 2, Tu ; (b) Turbulence level distribution along the jet axis, 1 to 6 relate to $Re = 460, 1180, 1970, 2620, 2810,$ and 4092 .

latter ones are formed at higher Reynolds numbers. The puffs are characterized by a smooth forward velocity front and a steep backward front, as distinct from the slugs having two steep fronts. An example of a structure of the puff type is presented in Fig. 4a. These data were obtained for the carbon dioxide outflow into the air using the high-speed PIV with the temporal resolution of 7 kHz (the flow is from top down). The value $Re = 2462$ corresponds to regime B. As can be seen from the time dependence of the longitudinal velocity component at the axis, the velocity is reduced throughout the entire puff region. As at the tube exit, the puff in the jet possesses a smooth leading front and a steep backward front, which is in agreement with the data for the tube flow [15]. In Fig. 4a it can also be seen that the puff in the jet has a complicated small-scale structure. The turbulent spot length and the frequency of its formation depend on the Reynolds number and the prehistory of its development within the tube.

It is known that laminar-turbulent transition in cylindrical channels occurs through the intermittence mechanism [15–17]. In this connection, we measured the intermittence coefficient γ in the near field of

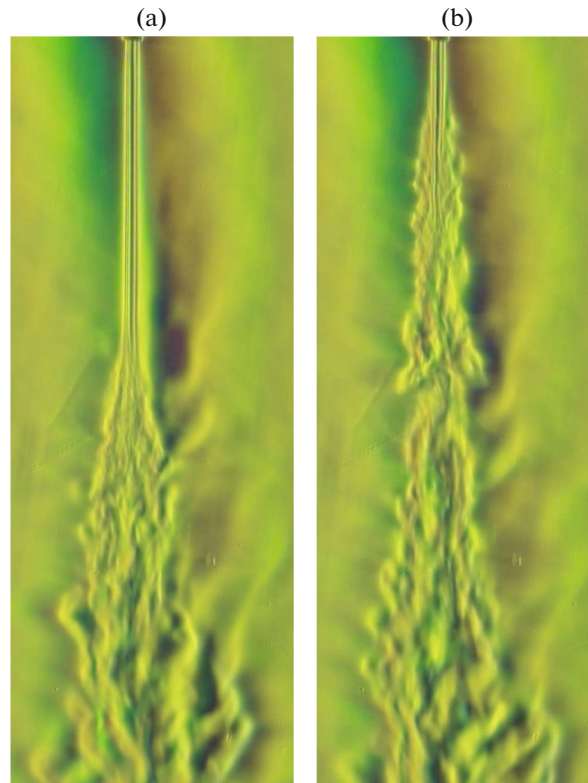


Fig. 3. Hilbert visualization of the outflow of Freon-22 (CHF_2Cl) jet into the air ($d = 2$ mm and $\text{Re} = 2853$); (a) jet in the absence of turbulent structures and (b) jet in the presence of turbulent puff.

the jet issuing from the tube. The intermittence coefficient is understood to mean the fraction of time, when velocity fluctuations are higher than a threshold value. The method of assessing γ on the basis of a time series proposed in [24] was applied. In Fig. 4b the dependence of the coefficient γ on the Reynolds number is presented for two gases, namely, propane (1) and air (2) at $x/d = 5$. As can be seen in the figure, $\gamma = 0$ for regime A, that is, the flow in the tube is laminar, and $\gamma = 1$ for regime B, when the tube flow is turbulent. The Reynolds number range, in which the intermittence coefficient γ is within the limits from 0 to 1, corresponds to regime B, that is, laminar-turbulent transition in the tube. The value $\gamma = 0.5$ corresponds to the case, in which the flow is laminar half the time and turbulent during the other half. As follows from Fig. 4b, the nature of variation of the coefficient γ in regime B is approximately the same for propane and air and is in agreement with the variation of this parameter in tube flows [15]. However, the least Reynolds number Re_1 , at which the intermittence coefficient becomes nonzero, and the value Re_2 , at which $\gamma = 1$, are different from the two gases. This can be attributed to the fact that in tube flows the critical Reynolds number is a function of many parameters and, in particular, Re_1 is sensitive to the initial disturbance level [15]. The limiting Reynolds number presented in the literature $\text{Re}_1 = 10^5$ [15]. In our experiments we used feeding gas manifolds (from the gas source to the tube inlet) of different design for propane and air, and the disturbance level at the tube inlet was not monitored.

From the results of the measurements in the jet near-field ($x/d < 40$) at $\text{Re} \sim 1900\text{--}3500$ we can conditionally separate two spatial zones, namely, near-axial and peripheral. In the axial zone laminar regions with low velocity fluctuation levels are chaotically alternated with turbulent spots with a high fluctuation level. The intermittent flow nature is observable throughout the entire near field. The general intermittence pattern qualitatively corresponds to the process of transition to turbulence observable in cylindrical channels [15]. In the downstream peripheral zone the Kelvin–Helmholtz instability was observed at the laminar flow stage; it is analogous to that developed in the mixing layer of jets flowing out of contoured confusers [3–6]. At the turbulent flow stage regions with puffs were recorded in this zone. The two zones join near the coordinate approximately corresponding to a velocity fluctuation maximum at the jet axis (Fig. 2b). The experimental data obtained in this zone demonstrate the remainders of turbulent spots, the

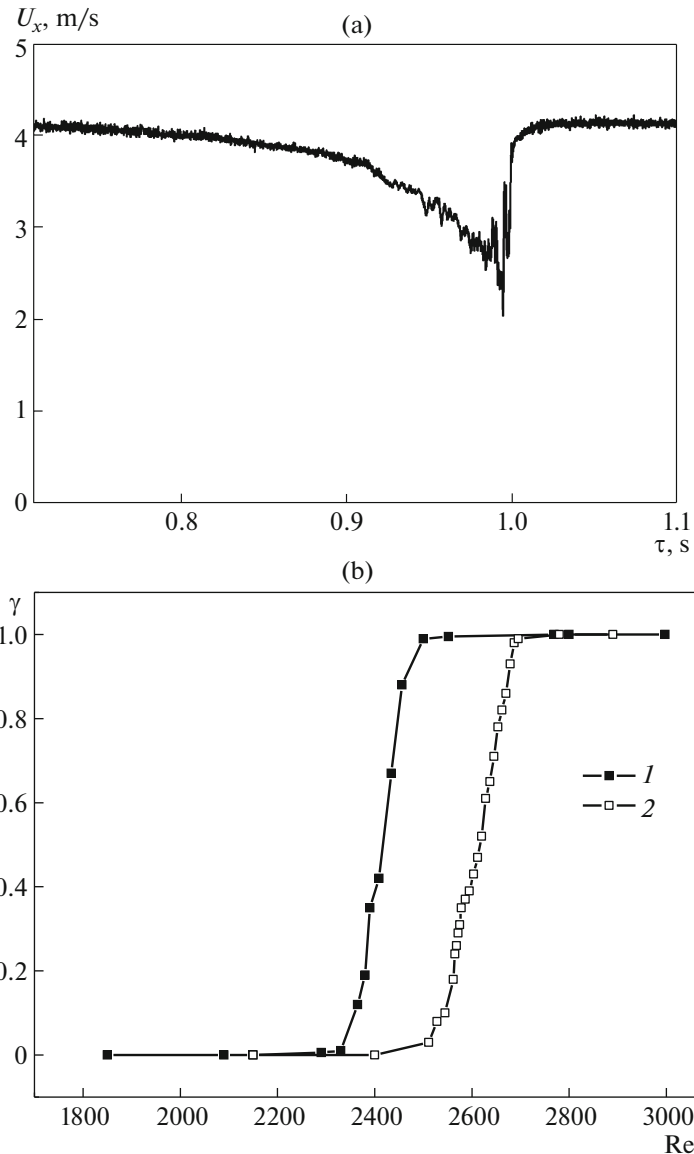


Fig. 4. Intermittence in the jet on transition to turbulence; (a) PIV measurements of the longitudinal velocity component in the turbulent puff at the jet axis ($d = 8$ mm, $x/d = 0.8$, and $Re = 2462$, the working gas is CO_2) and (b) intermittence coefficient distribution in the gas jet ($d = 3$ mm and $x/d = 5$): 1, propane and 2, air.

growing instability of Kelvin–Helmholtz waves, and the general growth of the broadband noise. The diagnostics of the vortex structures in this region is very difficult and requires for further investigation.

Thus, in the case of gas jet outflow from long axisymmetric channels transition to turbulence through the intermittence mechanism was recorded. This laminar-turbulent transition scenario is confirmed by means of varying different gases, the channel diameter, and the experimental methods of investigation. The main cause for this mechanism is laminar-turbulent transition in the jet source. The main structure unit of this process is represented by localized turbulent structures of the puff type. They are generated in tubes, are stable in the jet near-field, and break down in the region of transition to turbulence. This scenario is fundamentally different from the subharmonic scenario [3, 9] connected with the vortex coalescence phenomenon, which is well known for the outflow of jets from contoured nozzles (confusers).

3. REACTING JETS

The experiments with nonreacting jets make it possible to put forward some new possibilities of controlling the mixing and combustion processes in reacting jet flows at low Reynolds numbers ($Re < 4000$).

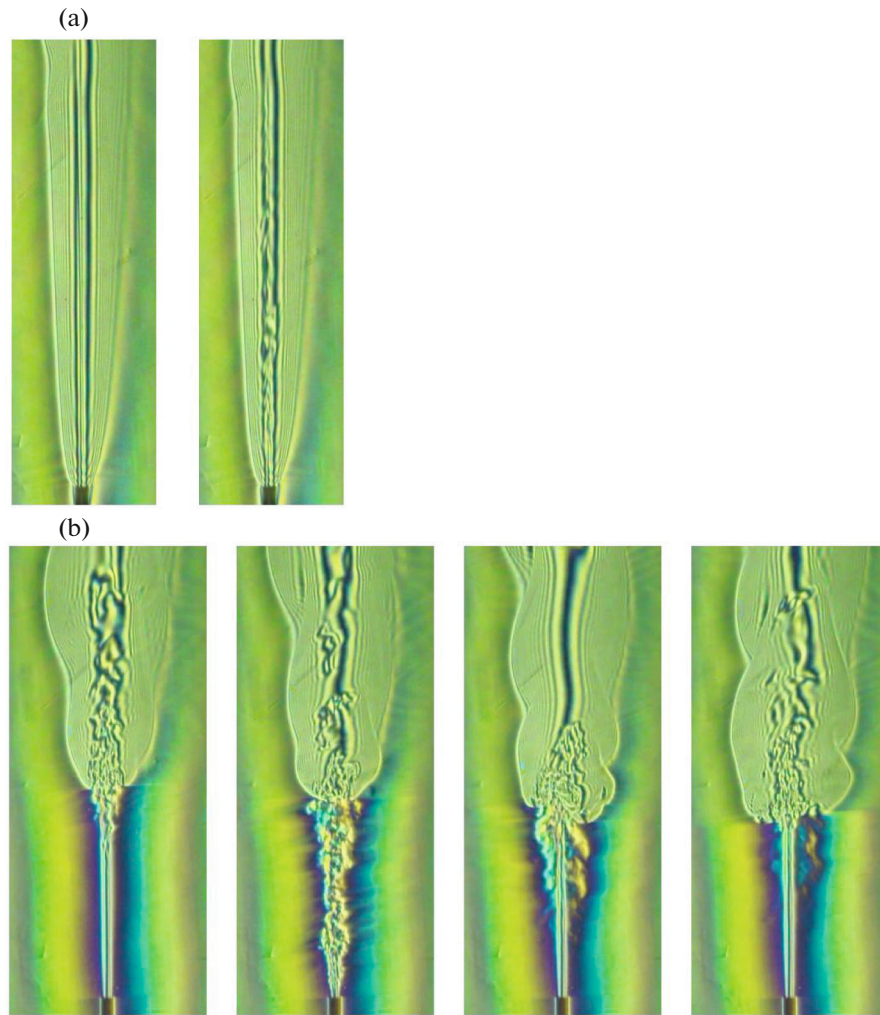


Fig. 5. Flow visualization in the case of diffusion combustion using the Hilbert optics, $d = 2.3$ mm, C_3H_8/CO_2 mixture, and $Re = 1980$; (a) attached flame, $Y = 25\%$ and (b) detached flame, $Y = 20\%$.

Since the mechanism of turbulence generation in a long tube is independent of the jet flow, this scenario of transition to turbulence through intermittence apparently exists also for jets with chemical reactions, in particular, in diffusion flames.

In Fig. 5 the Hilbert visualization images obtained during the propane jet combustion are presented flow from down top. The molar fraction of propane in its mixture with CO_2 $Y = 20\text{--}25\%$, which is considerably greater than the upper concentration limit of combustion of homogeneous propane-air mixtures (10.9%). This ratio ensured the conditions of the diffusion combustion regime with the formation of a flame front characteristic of a local heat release region. Figure 5a presents an attached flame for $Y = 25\%$, while in Fig. 5b the detached flame obtained at $Y = 20\%$ is shown. In both cases, successive snapshots are presented. For the case of the attached flame (Fig. 5a) localized structures are not observable in the axial region of the left frame; at the same time in the axial region of the right frame (Fig. 5b) a large-scale vortex structure, about $20d$ in length, is fixed. The structures in the axial region of a flame were also noticed in [18] but their identification was difficult in view of low spatial resolution of the images. Throughout the entire velocity range ($U_m = 0.8\text{--}9$ m/s) of the outflow of a submerged jet of pure propane the combustion is accompanied by low-frequency flicker oscillations of the plume, which are due to the action of buoyancy forces. These oscillations of the outer plume boundary are detectable at the tops of snapshots. However, any considerable influence of the puffs on the plume flicker density was not observed, although their action on the phase characteristics of the outward flame front oscillations was noticed. We note that disturbances do not almost propagate in the transverse direction, beyond the limits of the flame front (outward boundary of the plume).

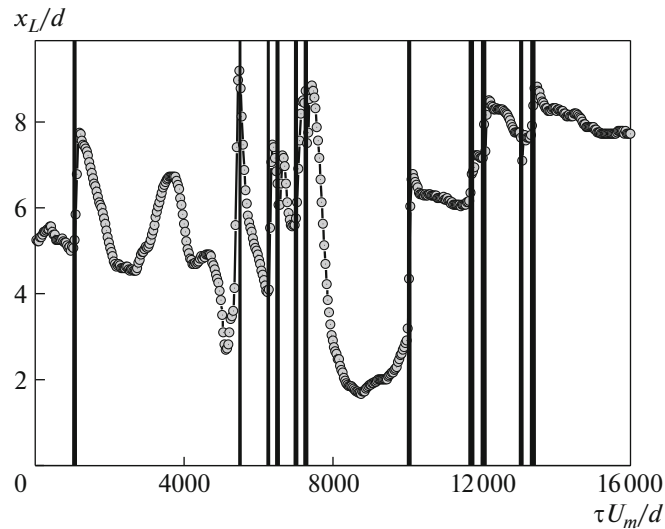


Fig. 6. Location of the forward front of the flame in C_3H_8/CO_2 as a function of time, $Y = 46\%$, $Re = 2966$, and $d = 3$ mm.

With increase in the air fraction in the combustion mixture the forward flame front is detached from the tube edge (four snapshots in Fig. 5b). In the first and fourth snapshots (from left to right) an extended laminar region without combustion can be observable. In the second and third snapshots the passage of a puff is recorded. In its downstream motion the puff is identified in both the region without combustion and the combustion zone. As can be seen in Fig. 5b, in the jet region, from the tube exit to the leading edge of the flame, the action of the structures leads, as in a nonreacting flow, to jet flow turbulization. During the puff motion in the combustion zone the leading front of the flame is considerably deformed. Apparently, the large-scale structures have an effect on the conditions of flame front stabilization, leading to a variation in the spatial flame topology.

An important characteristic of the detached flame, which determines, in particular, the conditions of flame extinction, is the position of the flame front x_L . The spatial dynamics of the detached flame as a function of x_L/d on the dimensionless time $\tau U_m/d$ is presented in Fig. 6. The appearance of a disturbance in the jet (vertical lines in Fig. 6) is preceded by a decrease in the velocity, which leads to the displacement of the leading edge of the flame upstream. After the disturbance has passed the velocity in the jet considerably increases and the flame front is displaced considerably downstream. This behavior of x_L is attributed to the nature of the variation in the longitudinal velocity within the puff structure (see Fig. 4a). It is known that a portion of natural disturbances decays within the tube, generating a small reduction in the velocity [15]. The x_L coordinate is also responsive to this disturbance (local minimum at $\tau U_m/d = 3636$) but on visualization of this disturbance a structure of the puff type is not observable. From the time series for the coordinate x_L the intermittence coefficient for the jet plume can be determined; in particular, for the experimental conditions presented in Fig. 6 $\gamma = 0.07$.

Comparing the flow dynamics in the near fields of the reacting and nonreacting jets the following conclusions can be made. The initial conditions in subsonic jets are caused by the flow development dynamics in axisymmetric channels. Here, the main parameters are the Reynolds number and the conditions at the tube entry. In particular, in the regime of laminar-turbulent transition in a long tube the intermittence process with the structures of the puff type are realized in the final section of the channel. These localized turbulent formations are stable in the near zones of both inert and reacting jets, which leads to the intermittence mechanism in jet flows. Further downstream, these vortex formations break up and transition to developed turbulent jet flow is realized. The reacting diffusion plumes (nonpremixed mixtures) possess an important peculiar feature in this scenario. This is due to the occurrence of chemical reactions and non-isothermal flow nature. In this case, the additional parameters are the composition of the combustion mixture and the ratio of its components. However, the initial conditions in the form of intermittence and the puff type structures also manifest themselves in flows with reactions.

In practice, the use of burners at relatively low Reynolds numbers ($Re < 4000$) means small values of velocities and fuel consumption. The jet outflow from long tubes makes it possible to obtain jets with long laminar zones [11, 12]. Thus, long-range jets can be produced in combustors at a smaller fuel consump-

tion. Another practically important regime is the use of the Reynolds number range characteristic of laminar-turbulent transition in long tubes, $Re = 1900\text{--}3500$. In this case, jet plumes can be controlled by means of introducing controlled disturbances at the tube entry [25]; in particular, they can be switched from the attached to the detached state and vice versa [19].

SUMMARY

In the case of outflow of inert and reacting jets from long axisymmetric channels a scenario of transition to turbulence through the intermittence mechanism is first revealed. The Reynolds numbers $Re = 1900\text{--}3500$ at which this mechanism occurs in the jet near-field, correspond to laminar-turbulent transition of gas flow within the channel.

It is shown that the reason for the intermittence is the occurrence of turbulent spots of the puff type. These localized turbulent structures are statistical in nature and are formed within long tubes in the absence of artificial disturbances. In the jet near-field the length of these structures is of the order of 20–30 tube diameters and they occupy the entire cross-sectional area of the jet. In the initial jet region the vortex formation are fairly stable and break down in the region of transition to turbulence.

The scenario revealed is considerably different from the widely known mechanism of laminar-turbulent transition for the jets issuing from the nozzles of confusor type, where the subharmonic wave mechanism due to vortex coalescence in the jet mixing layer is chiefly realized. The turbulent spots formed in the tube in the transitional regime can have a considerable effect on the dynamics of the free jet and the diffusion plume. Since the mechanism of turbulence generation in the jet is independent of the jet flow, this scenario of transition to turbulence through intermittence, apparently, exists for liquid jets and low-temperature plasmas.

FUNDING

The study is carried out within the framework of the State Assessment of the Institute of Thermophysics of the Siberian Branch of the Russian Academy of Sciences AAAA-A17-117030310010-9.

DECLARATION OF CONFLICTING INTERESTS

The Authors declare no potential conflicts of interest with respect to the research, authorship, and/or publication of this article.

REFERENCES

1. G. N. Abramovich, *Theory of Turbulent Jets* (MIT Press, Cambridge, 1963).
2. O. I. Navoznov, A. A. Pavel'ev, and A. V. Yatsenko, "The transition to turbulence in submerged jets and wakes," *Fluid Dynamics* **7**(4), 672–678 (1972).
3. C. M. Ho and P. Huerre, "Perturbed free shear layers," *Annu. Rev. Fluid Mech.* **16**, 356–424 (1984).
<https://doi.org/10.1146/annurev.fl.16.010184.002053>
4. A. Michalke, "Survey on jet instability theory," *Progr. Aerospace Sci.* **21**(3), 159–199 (1984).
[https://doi.org/10.1016/0376-0421\(84\)90005-8](https://doi.org/10.1016/0376-0421(84)90005-8)
5. A. S. Ginevsky, Y. V. Vlasov, and R. K. Karavosov, *Acoustic Control of Turbulent Jets* (Springer-Verlag, Berlin, 2004).
<https://doi.org/10.1007/978-3-540-39914-8>
6. V. V. Kozlov, G. R. Grek, and Yu. A. Litvinenko, *Visualization of Conventional and Combusting Subsonic Jet Instabilities* (Springer International Publishing, 2016).
<https://doi.org/10.1007/978-3-319-26958-0>
7. C. G. Ball, H. Fellouah, and A. Pollard, "The flow field in turbulent round free jets," *Progr. Aerospace. Sci.* **50**, 1–26 (2012).
<https://doi.org/10.1016/j.paerosci.2011.10.002>
8. I. V. Belyaev, O. P. Bychkov, M. Yu. Zaitsev, V. A. Kopiev, V. F. Kopiev, N. N. Ostrikov, G. A. Faranosov, and S. A. Chernyshev, "Development of the strategy of active control of instability waves in unexcited turbulent jets," *Fluid Dynamics* **53**(3), 347–360 (2018).
<https://doi.org/10.7868/S0568528118030027>
9. A. F. Hussain and K. Zaman, "The preferred mode of the axisymmetric mode," *J. Fluid Mech.* **110**, 39–71 (1981).
<https://doi.org/10.1017/S0022112081000608>

10. G. Nathan, J. Mi, Z. Alwahabi, G. Newbold, and D. Nobes, "Impacts of a jet's exit flow pattern on mixing and combustion performance," *Progr. Energy Combust. Sci.* **32**, 496–538 (2006).
<https://doi.org/10.1016/j.pecs.2006.07.002>
11. A. J. Reynolds, "Observations of a liquid-into-liquid jet," *J. Fluid Mech.* **14**, 552–556 (1962).
<https://doi.org/10.1017/S0022112062001433>
12. V. V. Lemanov, V. V. Terekhov, K. A. Sharov, and A. A. Shumeiko, "An experimental study of submerged jets at low Reynolds numbers," *Techn. Physics Lett.* **39**(5), 421–423 (2013).
<https://doi.org/10.1134/S1063785013050064>
13. Yu. S. Zaiko, A. I. Reshmin, S. Kh. Teplovodskii, and A. D. Chicherina, "Investigation of submerged jets with an extended initial laminar region," *Fluid Dynamics* **53**(1), 95–104 (2018).
<https://doi.org/10.7868/S0568528118010103>
14. J. Zayko, S. Teplovodskii, A. Chicherina, V. Vedenev, and A. Reshmin, "Formation of free round jets with long laminar regions at large Reynolds numbers," *Phys. Fluids* **30**, Art. No. 043603 (2018).
<https://doi.org/10.1063/1.5021017>
15. T. Mullin, "Experimental studies of transition to turbulence in a pipe," *Annu. Rev. Fluid Mech.* **43**, 1–24 (2011).
<https://doi.org/10.1146/annurev-fluid-122109-160652>
16. K. Avila, D. Moxey, A. De Lozar, M. Avila, D. Barkley, and B. Hof, "The onset of turbulence in pipe flow," *Science* **333**, 192–196 (2011).
<https://doi.org/10.1126/science.1203223>
17. N. V. Nikitin and V. O. Pimanov, "Sustainment of oscillations in localized turbulent structures in pipes," *Fluid Dynamics* **53**(1), 65–73 (2018).
<https://doi.org/10.7868/S0568528118010073>
18. F. Takahashi, M. Mizomoto, and S. Ikai, "Transition from laminar to turbulent free jet diffusion flame," *Combustion Flame* **48**, 85–95 (1982).
[https://doi.org/10.1016/0010-2180\(82\)90117-1](https://doi.org/10.1016/0010-2180(82)90117-1)
19. V. V. Lemanov, V. V. Lukashov, R. Kh. Abdrakhmanov, V. A. Arbuzov, Yu. N. Dubnishchev, and K. A. Sharov, "Regimes of unstable expansion and diffusion combustion in a hydrocarbon fuel jet," *Combustion, Explosion, Shock Waves* **54**(3), 255–263 (2018).
<https://doi.org/10.15372/FGV20180301>
20. R. C. Reid, J. M. Prausnitz, and T. K. Sherwood, *The Properties of Gases and Liquids* (McGraw-Hill, New York, 1977).
21. Yu. N. Dubnishchev, V. A. Arbuzov, P. P. Belousov, and P. Ya. Belousov, *Optical Methods of Flow Investigation* (Novosibirsk Univ. Press, 2003) [in Russian].
22. Y. N. Dubnishchev, V. A. Arbuzov, V. V. Lukashov, K. A. Sharov, and V. V. Lemanov, "Optical Hilbert Diagnostics of Hydrogen Jet Burning," *Optoelectron. Instrument. Proc.* **55**(1), 16–19 (2019).
<https://doi.org/10.3103/S8756699019010035>
23. S. V. Alekseenko, A. V. Bilsky, V. M. Dulin, D. M. Markovich, "Experimental study of an impinging jet with different swirl rates," *Int. J. Heat Fluid Flow* **7**, 1340–1359 (2007).
<https://doi.org/10.1016/j.ijheatfluidflow.2007.05.011>
24. C. L. Kuan and T. Wang, "Investigation of the intermittent behavior of transitional boundary layer using a conditional averaging technique," *Exp. Therm. Fluid Sci.* **3**(2), 157–173 (1990).
[https://doi.org/10.1016/0894-1777\(90\)90084-K](https://doi.org/10.1016/0894-1777(90)90084-K)
25. V. Lemanov, V. Lukashov, K. Sharov, and D. Nezavitin, "Turbulent spots in the flame of a diffusion torch," *J. Phys.: Conf. Ser.* **1382**, Art. No. 012058 (2019).
<https://doi.org/10.1088/1742-6596/1382/1/0120>

Translated by M. Lebedev